Across the Bridge: The Merrimack Undergraduate Research Journal

Volume 1 Article 9

2019

Using Complex Orthogonal Decomposition to Extract Dispersion Relationships for Mass Chain

Nicholas A. Valente
valenten@merrimack.edu

Rickey A. Caldwell
caldwellr@merrimack.edu

Using Complex Orthogonal Decomposition to Extract Dispersion Relationships for Mass Chain

Nicholas A. Valente

Dr. Rickey A. Caldwell Jr.

Abstract

Complex orthogonal decomposition (COD) was used to determine the extracted dispersion relationship of a traveling wave in a mass chain. When COD extracts a wavenumber it will produce M values for each wavenumber, γ_i*, and N values for each frequency,* ω_i*; where M is the number of masses and N is the number of time samples. In this work, least squares and a simple mean of the M-*γ_i*'s and N-*ω_i*'s extracted values were used to determine each* γ_i *and* ω_i*, respectively. An analytical dispersion relationship for the mass-chain is derived in addition to an approximate dispersion relationship. The approximate derivation was found using Lindstedt-Poincare's perturbation method. Lastly, the effects of the sampling rate on parameter′ extraction was studied. COD could accurately extract the wavenumber and frequency of a traveling wave in the mass chain. Using a simple mean provided marginally better results than that of least squares. Sampling at the Nyquist criterion gave accurate results which improved both marginally and asymptotically as the sampling rate increased.*

Keywords: *Complex Orthogonal Decomposition, dispersion relationships, mass chain*

Nomenclature

i	*Number of mass elements*
x	*Spatial Coordinate*
t	*Time (s)*
u	*Nondimensionalized spatial coordinate*
k	*Spring stiffness (N/m)*
h	*Relaxed length of each spring (m)*
γ	*Wavenumber (rad/m)*
ω	*Frequency (rad/s)*

α *There are two arguments for each entry of the nomenclature environment, the symbol and the definition*

ε *Perturbation parameter*

Introduction

Proper orthogonal decomposition (POD) was formulated by several researchers in the mid-twentieth century [1–3], and has many applications in engineering including the field of vibrations [4–6]. Within the field of structural vibrations POD has been used to estimate modal parameters with respect to standing waves. Complex orthogonal decomposition (COD) [7] is a specialized form of POD. COD [7] has been applied to traveling waves in elastic media [8] and in bio-locomotion [9–11] .

In the application of COD the practitioner typically starts with an ensemble of measured displacements. Then this matrix is converted into an ensemble of analytic signals using the Hilbert Transform. Next, the correlation matrix is computed from the ensemble matrix, and the eigenvectors and eigenvalues of the correlation matrix are determined. The eigenvectors of the correlation matrix are used to extract the corresponding wavenumbers. The eigenvectors and the ensemble matrix are used to compute the complex modal coordinates q_i which are used to estimate frequencies.

The relationship between frequencies and wavenumbers is called the dispersion relations [12]. Two other properties, phase velocity and group velocity, can be computed from the dispersion relationship. In this body of work, the wavenumbers and frequencies are extracted from a simulated mass-chain of 250 masses. The first mass had initial conditions $x_1(0) = x(0)$ and $\dot{x}_1(0) = 1$ which created a traveling wave propagating towards the 250th mass. The resulting displacements of each mass was captured before the wave reflection reached the 100th mass. To find an analytical dispersion relationship, an ordinary differential equation for the i^{th} mass was derived following [13] for linear springs only. The partial differential form of the equation is computed by taking the continuum limit of the ODE. The analytical form of the dispersion relationship is determined by substituting a solution of the wave equation into the PDE. The trial solution $y(x,t) = e^{i(\gamma x - \omega t)}$ resulted in a converging power series. Applying

Lindstedt-Poincairé's perturbation method to the ODE resulted in a linear approximation of the dispersion relationship that was identical to [14].

The COD extracted wavenumbers and frequencies were compared to both derived dispersion relationships. When applying least squares to estimate wavenumbers and frequencies using the dispersion relationship series,

$$\omega = \sqrt{\sum_{n=1}^{\infty} \frac{2(-1)^{n+1}\gamma^{2n}}{2n!}},$$

to $n = 6$ as the actual value, the residual sum of squares error (RSSE) was 0.0655 and for using the means for parameter estimation the RSSE was 0.0088.

The paper contributes to the body of knowledge by finding an analytical dispersion relationship for a linear mass chain, quantifying the effects of temporal sampling on error and independently verifying findings in the literature.

Mathematics

The governing equation for a 250 mass-spring chain was derived from first principles. Physics for the i^{th} mass is governed by the spring and the mass of its nearest neighbors, as shown in Fig 1. Assuming each spring is: a linear ideal spring, has a stiffness of $k = 1\ \left(\frac{N}{m}\right)$, massless and is governed by Hooke's Law. Each mass x_i, has a mass of and is restricted to movement on the x-axis. Applying Newton's Second Law, the equation of motion for the i^{th} element is

$$m\ddot{x}_i = kx_{i+1} + kx_{i-1} - 2kx_i \tag{1}$$

An equation describing the continuum of coupled conservative oscillators was used to begin the process

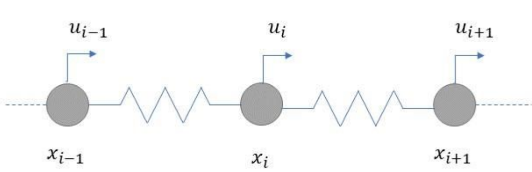

Fig. 1. Linear Mass Chain

of developing a dispersion relationship equation. The expression that appears in Eqn. (2) is the linear equation of Eqn. (1), where u describes the displacement of the i^{th} mass for the dynamical system.

$$\frac{\partial^2 u_i}{\partial t^2} = u_{i+1} + u_{i-1} - 2u_i \tag{2}$$

The passing of the continuum limit occurs when ordinary differential equations are replaced by partial differential equations. In doing so, the displacement of each mass can then be approximated utilizing a Taylor Series expansion. Express u in terms of both the spatial parameter x and time t; such that, $u_i(t) = u(x_i, t)$, $u_{i+1}(t) = u(x_{i+1}, t)$, and noting that $x_{i+1} - x_i = h$ [13]. Expanding these using the Taylor series to the fourth order yields:

$$\begin{aligned} u_{i+1} &= u_i + \frac{\partial u}{\partial x}\frac{h}{1!} + \frac{\partial^2 u}{\partial x^2}\frac{h^2}{2!} + \frac{\partial^3 u}{\partial x^3}\frac{h^3}{3!} + \frac{\partial^4 u}{\partial x^4}\frac{h^4}{4!} + O(h) \\ u_{i-1} &= u_i - \frac{\partial u}{\partial x}\frac{h}{1!} + \frac{\partial^2 u}{\partial x^2}\frac{h^2}{2!} - \frac{\partial^3 u}{\partial x^3}\frac{h^3}{3!} + \frac{\partial^4 u}{\partial x^4}\frac{h^4}{4!} + O(h) \end{aligned} \tag{3}$$

where h is defined as the relaxed length of each spring. Substituting both equations of Eqn. (3) into Eqn. (2), while creating a new variable $\tilde{x} = x/h$ and applying the chain rule leads to the following partial differential equation (note the tildes were omitted):

$$\frac{\partial^2 u_i}{\partial t^2} = 2\sum_{n=1}^{\infty} \frac{\partial^{2n} u}{\partial x^{2n}}\frac{1}{2n!} \tag{4}$$

From Eqn. (4), a trial solution Eqn. (5), which satisfies the wave equation, can be used to derive an equation for the dispersion relationship.

$$u(x,t) = e^{i(\gamma x - \omega t)} \tag{5}$$

This results in the expression of frequency ω in terms of wavenumber γ

$$\omega = \sqrt{\sum_{n=1}^{\infty} \frac{2(-1)^{n+1}\gamma^{2n}}{2n!}}, \tag{6}$$

Dispersion Relationship Linstedt-Poincaré

Perturbation theory is used to solve equations that describe varying dynamical systems. Notably, Linstedt-Poincaré's method is used to solve systems that have periodic solutions. The higher expansion´ of the computed solution tend to produce secular terms or terms that grow without bounds. Taking the simplified equation for the mass chain, Eqn. (2), and rewriting it to form an ordinary differential equation becomes

$$\frac{d^2u_i}{dt^2} = u_{i+1} + u_{i-1} - 2u_i \tag{7}$$

The expanded power series ω is expressed in terms of both ε and α, where values of ε are assumed to be small in magnitude and values for α are to be solved.

$$\omega = 1 + \alpha_1\varepsilon + \alpha_2\varepsilon^2 + O(\varepsilon) \tag{8}$$

Differentiating the linear relationship $\tau = \omega t$ twice and instituting a change of variables into Eqn. (7) leads to

$$\frac{d^2u_i}{d\tau^2}\omega^2 = u_{i+1} + u_{i-1} - 2u_i \tag{9}$$

The individual components that consist within the difference equation with respect to t are defined as

$$\begin{aligned} u_i(t) &= u_{i,0} + \varepsilon u_{i,1} + \varepsilon^2 u_{i,2} + O(\varepsilon) \\ u_{i+1}(t) &= u_{i+1,0} + \varepsilon u_{i+1,1} + \varepsilon^2 u_{i+1,2} + O(\varepsilon) \\ u_{i-1}(t) &= u_{i-1,0} + \varepsilon u_{i-1,1} + \varepsilon^2 u_{i-1,2} + O(\varepsilon) \end{aligned} \tag{10}$$

Squaring Eqn. (8) and substituting Eqn. (10) into Eqn. (9) yields equations that can be grouped in sequential levels of magnitude with respect to ε

$$\varepsilon^0 : \ddot{u}_{i,0} = u_{i+1,0} + u_{i-1,0} - 2u_{i,0} \tag{11}$$
$$\varepsilon^1 : \ddot{u}_{i,1} = u_{i+1,1} + u_{i-1,1} - 2u_{i,1} - 2\alpha_1 \ddot{u}_{i,0}$$
$$\varepsilon^2 : \ddot{u}_{i,2} = u_{i+1,2} + u_{i-1,2} - 2u_{i,2} - 2\alpha_1 \ddot{u}_{i,1} - 2\alpha_2 \ddot{u}_{i,0} - \alpha_1^2 \ddot{u}_{i,0}$$

Taking the first order approximation with respect to ε and inputting the trial solution Eqn. (5) for $u_{i,0}$ while defining $u_{i\pm1} = e^{\pm i\gamma} A e^{i(\gamma x - \omega t)}$ will result in a dispersion relationship for ω in terms of γ.

$$\omega = \sqrt{2\,(1 - \cos cos\,\gamma\,)} \tag{12}$$

This is compared to the analytical dispersion relationship extracted using Eqn. (6). This results are shown in Fig 2.

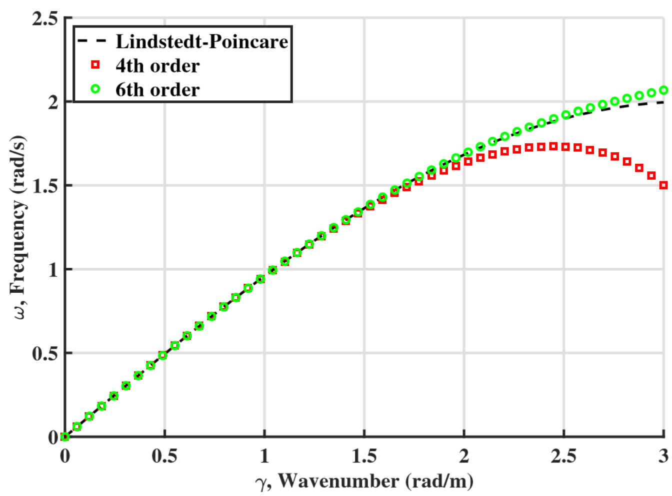

Fig. 2. Comparison of analytical dispersion relations. The dashed black line was computed using the ε equation from the Lindstedt-Poincaré perturbation. The square was computed from the 4th order approximation´ using equation 6 and the circle was computed from the 6th order approximation.

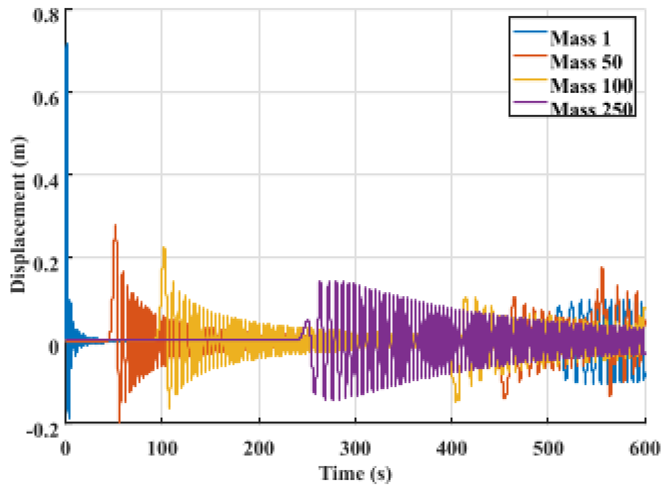

Fig. 3. The displacement time histories are shown for masses 1, 50, 100, and 250. The reflection of the traveling wave can be seen returning to mass 100 around t = 400.

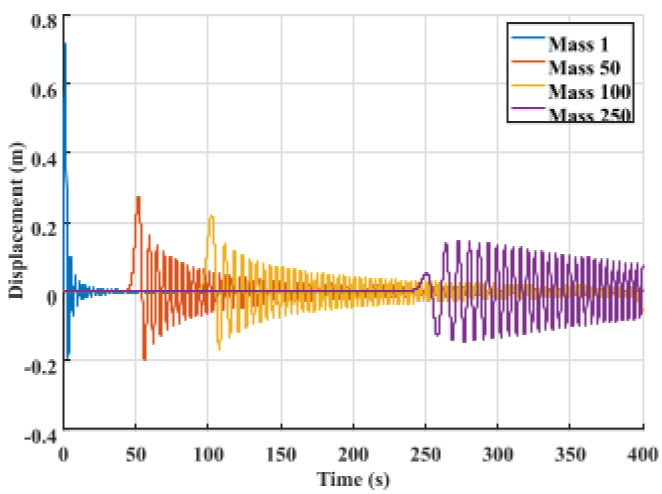

Fig. 4. The displacement of selected masses 1, 50, 100, 250

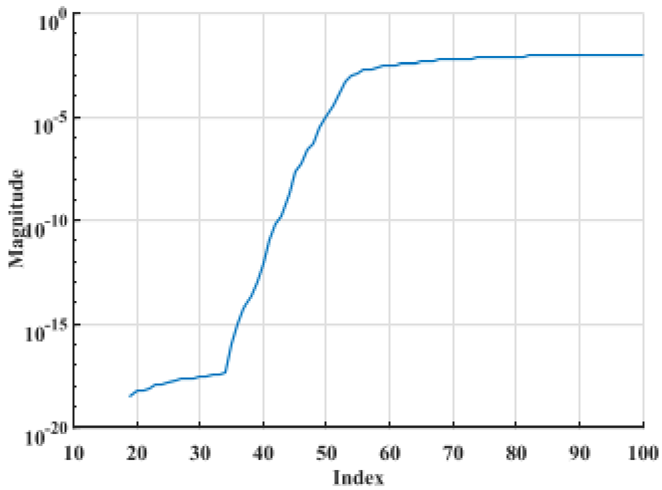

Fig. 5. Complex orthogonal values (COV) for the first 100 masses

Simulations

A 250 mass chain consisting of ideal linear springs was excited using initial condition $x_1(0) = 0$ and $\dot{x}_1(0) = 1$. The deflection of each mass was simulated using MATLAB *lsim* command. The responses were captured until the traveling wave reflection reached the 100th mass as shown in Fig 3, which took approximately 400 seconds. The response for $t \in [0, 400]$ was captured and used for extraction purposes, which is shown in Fig 4.

Complex Orthogonal Decomposition

The displacement measurements of the first 100 masses were used to form an ensemble matrix **X**, where **X** is an M by N matrix consisting of real elements. The constants M and N are defined by the number of masses in the system and the number of samples respectively. Performing the Hilbert Transform on each column of **X**, creates a signal that is both analytic and complex, meaning that the signal does not have negative frequency content. The new analytic ensemble of displacements is $H(X) = Z$. Using the complex ensemble matrix $Z \in C^{M \times N}$, a complex correlation matrix R is formed by computing

$$R = \frac{ZZ^H}{N} \tag{13}$$

where H is the complex conjugate transpose also known as the Hermitian transpose. Following the calculation of R, the eigenvalue problem is posed as

$$R\psi = \lambda\psi \tag{14}$$

The eigenvalues, λ, are called complex orthogonal values (COV) and the eigenvectors, ψ, are denoted as the complex orthogonal modes (COM) [7]. Figure 5 displays the COVs for the first 100 eigenvectors. COVs are used to discern spurious eigenvectors from ones suitable for parameter extraction. The higher magnitude COVs have smooth circular COMs associated with them, and as magnitude decreases the COM becomes more jagged and angular. This can been seen in Fig 6. It can be seen in Fig. 5 that the 60th eigenvector and higher are suitable for parameter extraction [7,14].

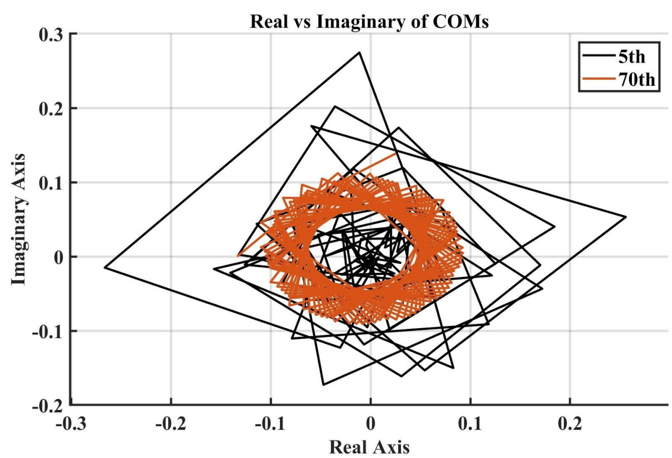

Fig. 6. Example of COM's with a Low Magnitude COV (Blue) and High Magnitude COV (Orange)

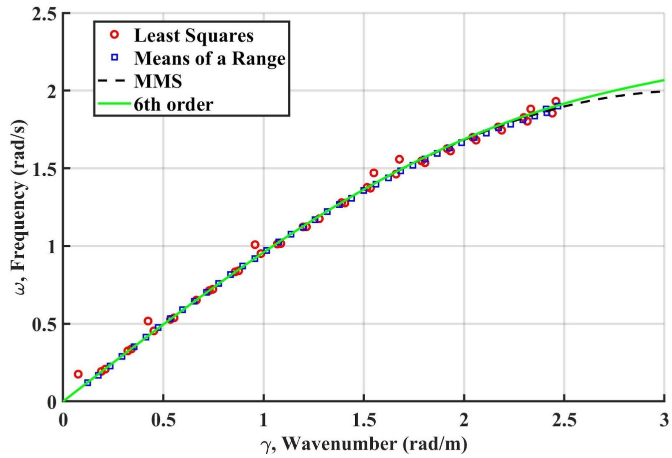

Fig. 7. Dispersion Relationship for Least Squares Approximation, Mean of a Range, Method of Multiple Scales, and 6th Order Lindstedt-Poincaré

Having identified the eigenvectors to choose, a wavenumber from each eigenvector can be extracted. The, wavenumber γ_i is extracted using $\gamma_i = \frac{\partial\angle(\psi_i)}{\partial x}$. Complex modal coordinates **Q** can be found by $Q = \Psi^{-1}X$. Hence, the values for frequency are then found by $\omega_i = \frac{\partial\angle(q_i)}{\partial t}$. Figure 7 is the dispersion relationship used by taking the means of all data point produced by COD. It can be seen that this does not provide a good fit to the theoretical curve. This is due to some of the data being produced when the wave has not yet reached the mass or has passed the mass. This can be seen in Fig 8 where the data is extracted from the part of the phase that has a slope. Using this range, it can be said that these values agree well with the theoretical dispersion relationship, as shown by the black squares that appear in Fig 7. Parameter estimations from the COD extracted values will be explored in greater details in the next section.

Parameter Estimation

To explore increasing the accuracy of the dispersion relationship estimations, two methods were investigated: Least Squares and simple mean. Figure 8 displays the phase angle that comes as a result of unwrapping the complex modal coordinates **Q**. For each γ_i, COD will provide M extracted data points and for ω_i up to N data points. The least squares method was to fix data from the unwrapped phase to $phase(x) = \gamma x$ for estimate

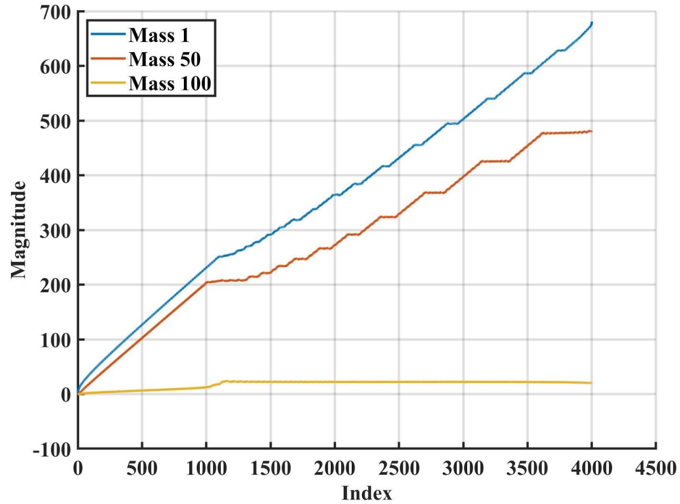

Fig. 8. Phase Angle Magnitudes of Selected Complex Modal Coordinates

Tab. 1. RSSE vs Sampling Frequency

Frequency (Hz)	RSSE Means	RSSE Least Squares
10	0.0088	0.0655
25	0.0092	0.0402
50	0.0096	0.0405
100	0.0103	0.0309
150	0.0103	0.0360
200	0.0106	0.0309

the wavenumber and $phase(t) = \omega t$ to estimate the frequency. In addition to the parameter estimation using Least Squares, the wavenumbers and frequencies were estimated by taking the mean of the partial derivatives of the phase angle with respect to time and the spatial variable x, respectively. This resulted in the formation of a second dispersion relationship extraction. Figure 7 shows the dispersion relationships using the means of all data extracted by COD (green), mean of portion of the data when the traveling wave is present (black), and the least squares of the selected data. When using the residual sum square error (RSSE) as a metric both the means and the least squares dispersion relationship have small error. The RSSE values for each parameter estimation method is shown in Tab 1. Additionally, the sampling rate was increase to see if it had an effect on accuracy. The parameter estimation using COD is insensitive to temporal sampling as seen in Fig 9.

Discussion and Results

The goal of this research was to apply the complex orthogonal decomposition method to a simulated mass-chain and extract the wavenumber in conjunction with frequencies of traveling wave propagating in the mass-chain. To evaluate accuracy of the parameter extractions, the dispersion relationship for the mass-chain was determined and used as a metric.

To determine the dispersion relationship, a discrete lumped-mass model was created for the i^{th} mass, which was an ODE. This was converted to a continuous PDE by passing the continuum limit.

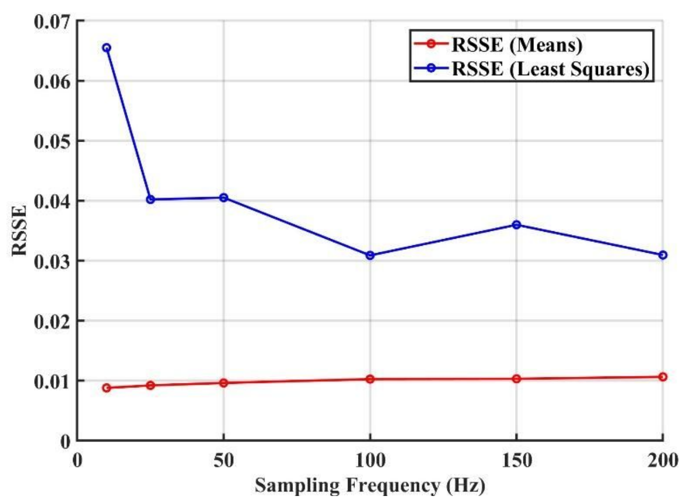

Fig. 9. Residual Sum Square Error (RSSE) versus Sampling Frequency (Hz) for Range of Means and Least S quares Parameter Extraction

A solution to the wave equation, $y(x, t) = e^{i(\gamma x - \omega t)}$, was substituted in the PDE which lead to the dispersion relationship in the form of a power series where, $\omega = \sqrt{\sum_{n=1}^{\infty} \frac{2(-1)^{n+1}\gamma^{2n}}{2n!}}$. This is a contribution to the body of research conducted. Additionally, another form of the dispersion relationship was formed by using Linstedt-Poincaré's perturbation method, resulting in an approximation

$\omega = \sqrt{2(1 - \cos cos\, \gamma\,)}$, which agrees with findings in literature.

Upon applying COD to the simulated responses of the masses in the mass-chain, the practitioner will have *M* extractions of each wavenumber and *N* extractions for each frequency. Typically, the mean of these extractions are used for the final parameter estimation. This work compared the results of using least squares or merely taking the means. The results for both were accurate, the RSSE for least square was 0.066 and 0.009 when taking the means. It can be seen that taking means was better and this is due to the occasional outlier when using least squares which can be seen in Fig 7. Also, when exploring how sensitive COD is to the sampling rate, it was determined that COD is insensitive to sampling and the RSSE converges asymptotically as Δt decreases. Phase velocity and group velocity were determined as additional characteristics of the structure. Group velocity is velocity of overall packet of waves and is determined by $c_g = \frac{\partial\omega}{\partial\gamma}$ for the linear mass chain that is

$$c_g = \frac{\sqrt{2}\,\sin sin\,\gamma}{2\sqrt{1-\cos cos\,\gamma}} \qquad (15)$$

Phase velocity is the velocity of a crest in the travel traveling wave and is defined as $c_p = \frac{\omega}{\gamma}$ for the mass chain it is

$$c_p = \frac{\sqrt{2-2\cos cos\,\gamma}}{\gamma} \qquad (16)$$

Perturbation methods gave an approximate solution in the neighborhood of the dynamical system. The dispersion relationship that came as a result of this approximate solution, was compared to [14].

The dispersion relationships were plotted to give a visual as to how the COD model compared to the analytic theory while, alternative methods of parameter extraction were also explored.

As aforementioned, COD has been applied as tool to deconstruct the bio-locomotion of nematodes and fishes [9–11]. New applications of COD include sensors for nondestructive evaluation. Additionally, mass-chains or meta-material structures could be embedded into products to differentiate genuine products from counterfeits. Verification can be determined by a device, which utilizes COD and travelling waves as a measure of authentication. Finally, one could exploit dispersion relationships of mass chains to create physical keys or encryption devices.

Further investigations of this work include: adding a nonlinear element to each spring and allocating specific spring stiffness for wave-guide design.

Acknowledgements

This paper has been submitted for conference publication in accordance with ASME-IDETC 2019.

References

[1] Kosambi, D., 1943. "Statistics in function space". *Journal of Indian Mathematical Society,* 7, pp. 76–88.

[2] Berkooz, G., Holmes, P., and Lumley, J. L., 1993. "The proper orthogonal decomposition in the analysis of turbulent flows". *Annual reviews of Fluid mechanics,* 25, pp. 539–575.

[3] Lumley, J., 1970. *Stochastic Tools in Turbulence*. New York, Academic Press.

[4] Chatterjee, A., April 2000. "An introduction to the proper orthogonal decomposition". *Current Science,* 78 (7), pp. 808–817.

[5] Feeny, B. F., and Kappagantu, R., 1998. "On the physical interpretation of proper orthogonal modes in vibrations". *Journal of Sound and Vibration,* 211(4), pp. 607–616.

[6] Azeez, M. F. A., and Vakakis, A. F., 2001. "Proper orthogonal decomposition (pod) of a class of vibroimpact oscillations,". *Journal of Sound and Vibration,* 240((5)), pp. 859–889.

[7] Feeny, B. F., 2013. "Complex modal decomposition for estimating wave properties in onedimensional media". *Journal of Vibration and Acoustics,* 135(3), p. 031010.

[8] Caldwell Jr, R. A., and Feeny, B. F., 2016. "Characterizing wave behavior in a beam experiment by using complex orthogonal decomposition". *Journal of Vibration and Acoustics,* 138(4), may, p. 041007.

[9] Feeny, B. F., and Feeny, A. K., 2013. “Complex modal analysis of the swimming motion of a whiting”. *Journal of Vibration and Acoustics,* 135(2), p. 021004.

[10] Feeny, B. F., Sternberg, P., Cronin, C., and Coppola, C., 2013. “Complex orthogonal decomposition applied to nematode posturing”. *Journal of Computational and Nonlinear Dynamics,* 8(4), p. 041010.

[11] Zuo, C., Xingshi, G., Kangkang, L., and Hongzhou, J., 2017. “Cfd studies of the effects of wave form on swimming performance of carangiform fish.”. *Applied Sciences (2076-3417),* 7(2), p. 149.

[12] Graff, K. F., 1975. *Wave motion in elastic solids*. Courier Dover Publications.

[13] Rand, R. H., 2012. “Lecture notes on nonlinear vibrations”.

[14] Caldwell, R. A., Panigrahi, S., and Feeny, B. F., 2016. “Extraction of wave dispersion characteristics in a discrete chain using complex modal decomposition”. In *Special Topics in Structural Dynamics, Volume 6*. Springer International Publishing, pp. 205–210.